

## An $^{18}\text{O}$ Tracer Study on the Growth Mechanism of Alumina Scales on NiAl and NiAlY Alloys

E. W. A. Young\* and J. H. W. de Wit†

Received February 21, 1986

---

*The effect of Y additions on the oxidation mechanism of NiAl at 1270 K has been investigated. Mass transport in the alumina scale was examined with  $^{18}\text{O}$  tracers. Proton activation analysis ( $^{18}\text{O}(p, \alpha)^{15}\text{N}$ ) and SIMS were used to measure the  $^{18}\text{O}$  distribution in the scale. On pure NiAl and low-doped (0.07% Y) NiAl mainly outward scale growth was observed. Addition of 0.5% Y induces oxide formation at both interfaces of the scale. Larger quantities of Y added to the alloy (> 0.5%) do not dissolve completely in the NiAl, but form Y-rich segregates. Internal oxidation of these intergranular segregates was observed. The relation between the modification of the scale-growth mechanism and the improved adherence of the scale to the alloy due to the addition of Y is discussed.*

---

**KEY WORDS:** high-temperature oxidation;  $\text{Al}_2\text{O}_3$ ;  $^{18}\text{O}$  tracers; oxidation mechanism

### INTRODUCTION

Spalling of the protective alumina scales on high-temperature alloys or coatings reduces considerably the lifetime and the applicability of these materials. It is well-known that the adherence of the scales can be improved by the addition of a small amount of rare-earth metals to the alloy. A

\*Inorganic Chemistry Department, State University Utrecht, Croesestraat 77A, 3522 AD Utrecht, The Netherlands.

†Laboratory for Metallurgy and Materials Science, Delft University of Technology, Rotterdamseweg 137, 2628 AL Delft, The Netherlands.

number of mechanisms have been proposed over the years to explain the beneficial effect of these additions.<sup>1</sup>

It has been reported in the literature that alumina scales grow by an inward growth mechanism due to oxygen transport along grain boundaries in the oxide. Also aluminum diffusion along short-circuit diffusion paths has been reported to contribute to the mass transport through the scale during high-temperature oxidation. In general the "rare-earth" effect has been discussed with modifications as to the character and relative importance of these diffusion paths.<sup>1,2,3,4</sup> In a recent <sup>18</sup>O tracer study we demonstrated that at 1420 K, Al and O are both mobile species, indeed, in the Al<sub>2</sub>O<sub>3</sub> scale at this temperature. At 1170 K however, outward scale growth was observed. Thus, it was concluded that at this relatively low temperature, Al transport through the scale predominates.<sup>5</sup>

The present study was undertaken to study the effect of Y additions on the transport of Al and O through alumina scales. To this end we investigated the oxidation mechanism of NiAl and of Y-doped NiAl alloys at 1270 K. <sup>18</sup>O tracer was used again to study the oxygen transport through the scale.

## EXPERIMENTAL

Buttons of pure NiAl and NiAl doped with Y (0.07, 0.5, and 1.0 wt.%) were produced by induction heating of appropriate metal powder mixtures in Argon. Slices of the obtained buttons were polished to a 1 μm finish. Oxidation was performed by alternating oxidation in flowing natural oxygen gas (hereafter referred to as <sup>16</sup>O) and in a sealed ampoule with <sup>18</sup>O-enriched (50%) oxygen gas (hereafter referred to as <sup>18</sup>O), as described previously.<sup>5</sup> The samples were slowly cooled and heated to avoid spalling of the scales. In all cases samples of NiAl and NiAlY alloys were oxidized in the same run, thus excluding pretreatment differences.

The <sup>18</sup>O tracers in the alumina scales were profiled by making use of the nuclear reaction <sup>18</sup>O(*p*, α)<sup>15</sup>N. The single-spectrum method was followed.<sup>5,6</sup> Samples were bombarded with a monochromatic beam of 800 keV protons, and the resultant α particles were detected at an angle of 170° to the proton beam. In addition to these proton-activation profile measurements, dynamic SIMS analyses were also performed in a CAMECA IMS 3F ion microscope. A Cs<sup>+</sup> source was used to erode the surface, and positive ions were detected. To avoid charging of the alumina scale the surface was gold coated, and during sputtering an electron flood was spread over the surface. Several selected masses could be monitored simultaneously in the assembly. Some of the alumina scales were examined by glancing angle X-ray diffraction<sup>9</sup> to obtain information about the oxide crystal structure.

Finally,  $^4\text{He}^+$  Rutherford Backscattering Spectrometry (RBS) measurements<sup>8</sup> and microscopic observations were performed.

## RESULTS

The NiAl1%Y alloy is a two-phase alloy, as can be seen in Fig. 1. Wavelength dispersive electron microprobe analysis showed that the intergranular phase contains most of the Y. Its composition is 47% Ni, 39% Al, and 14% Y (at.%). Optical micrographs of transverse sections of the scales (polished at 30° angle) show that there is severe oxidation along these second-phase segregates. A micrograph that clearly shows macropegs in the alloy is shown in Fig. 2. These oxide pegs contribute to the overall  $^{18}\text{O}$  depth distribution as measured. Without detailed knowledge of the lateral distribution of the  $^{18}\text{O}$  tracer, interpretation of depth profiles of oxygen might be erroneous.<sup>10</sup> Therefore the 1% Y alloy was not studied any further. The 0.5% Y-doped alloy has some very small regions of second-phase segregates as well. However, the contribution to the overall depth distribution of oxygen isotopes of the oxide pegs in these few and very small regions

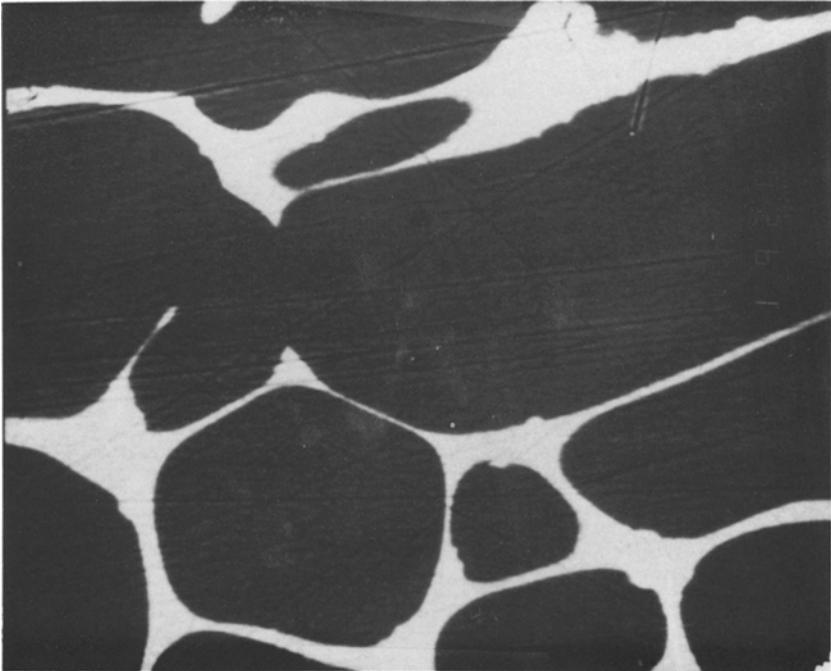


Fig. 1. SEM micrograph (BEI) of NiAl1%Y alloy (polished surface).

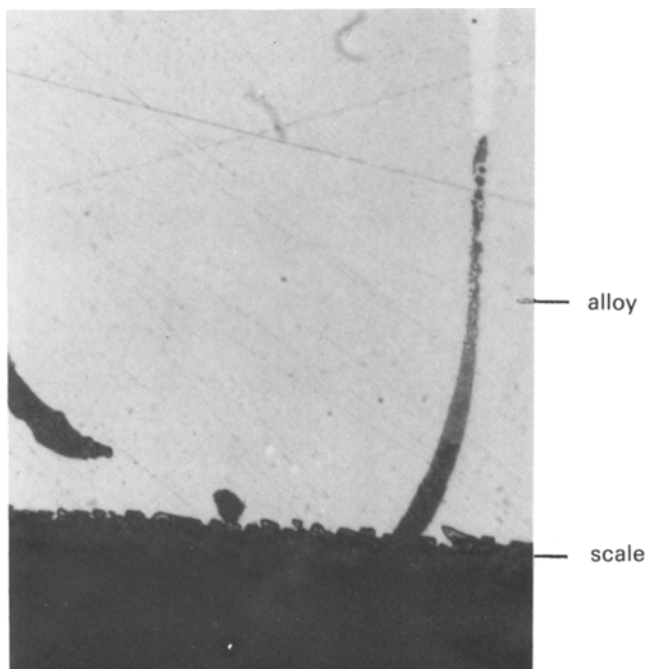
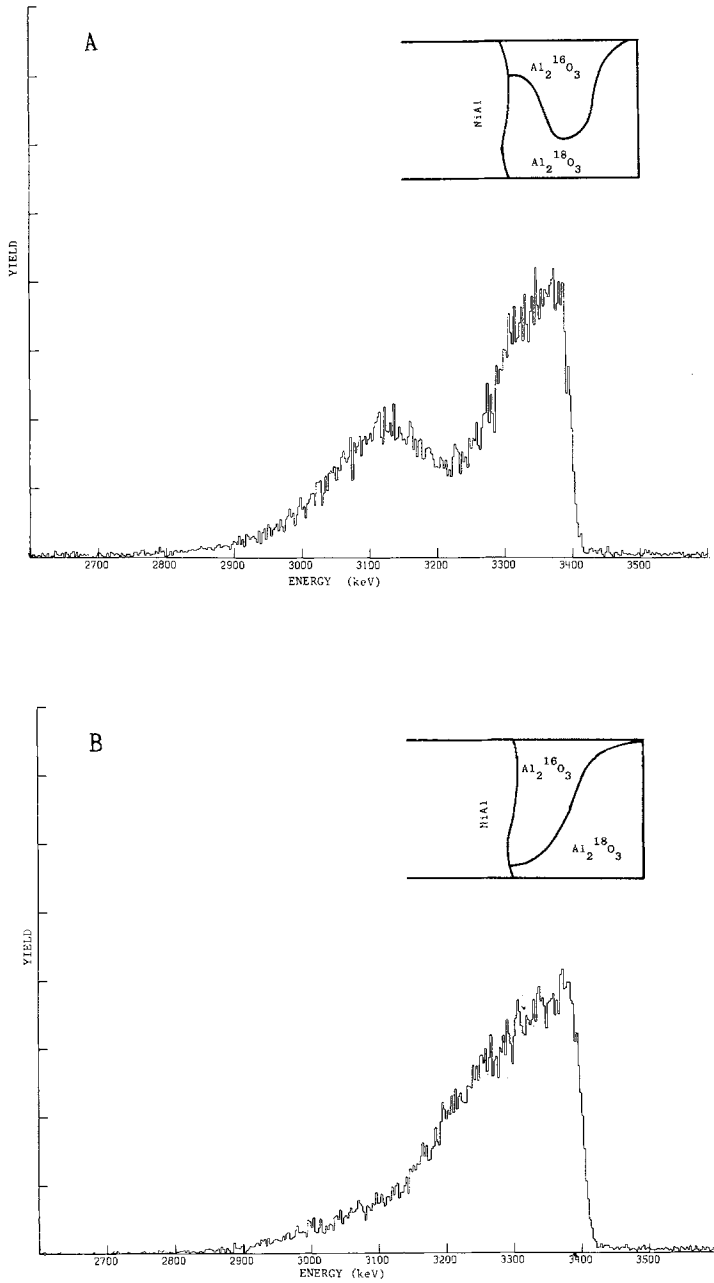


Fig. 2. Micrograph of a cross-section (30 A) of NiAl1%Y, oxidized for 7 hr at 1270 K.

can be neglected. NiAl and NiAl doped with 0.07% Y doped are single-phase alloys. These single-phase alloys and the 0.5% Y-doped alloy were selected for further investigation. Some results of the proton-activation measurements on these alloys are shown in Fig. 3. The spectra show the energy distribution of the  $\alpha$  particles leaving the specimen during bombardment with 800 keV protons (at  $170^\circ$ ). The spectra were obtained from specimens after oxidation first in  $^{16}\text{O}$  for 1.5 hr and later in  $^{18}\text{O}$  for 5.5 hr at 1270 K. The concept of proton activation profiling of  $^{18}\text{O}$  and the interpretation of the spectra will be given here briefly. A more detailed description of the technique, including the relevant aspects in oxidation studies, has been given before.<sup>5</sup>

During bombardment of the specimen with protons, most protons penetrate into the material. Some of the particles will collide with  $^{18}\text{O}$  nuclei. A reaction between an 800 keV proton and an  $^{18}\text{O}$  nucleus produces an  $\alpha$  particle with an energy of 3.4 MeV (if scattered at  $170^\circ$ , our angle of detection). However, if the reaction takes place below the surface, the  $\alpha$  particle will lose some energy on its way out of the material. The energy



**Fig. 3.**  $\alpha$ -spectrum (800 keV protons) of alloys oxidized first for 1.5 hr in  $^{16}\text{O}$ , later for 5.5 hr in  $^{18}\text{O}$  at 1270 K (A) NiAl0.5%Y; (B) NiAl0.07%Y; (C) NiAl (pure).

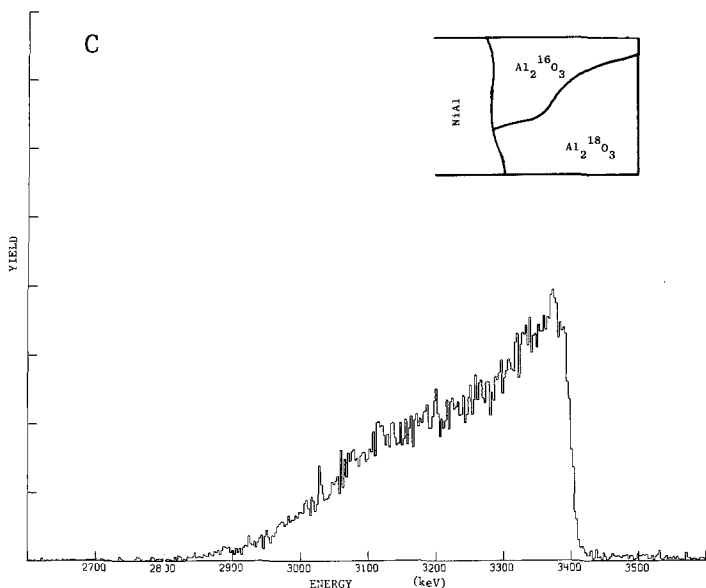


Fig. 3 Continued.

distribution of the  $\alpha$  particles can therefore be used for the depth profile of  $^{18}\text{O}$ . The energy of the  $\alpha$  particles varies almost linearly on the depth of the reaction. The yield of the  $\alpha$  particles gradually decreases with increasing depth, because the reaction cross-section decreases with decreasing proton energy. (Also the protons are retarded on their way through the material.)

The edge in the spectra at 3.4 MeV indicates that there is  $^{18}\text{O}$ -rich oxide at the surface of the alumina scale. In the alumina scales on NiAl and NiAl0.07% Y, the amount of  $^{18}\text{O}$  in the oxide decreases with depth below the surface (lower energy). Schematic representations of the oxygen distribution in the scales are given in the upper right corner of the spectra in Fig. 3. The representations given are in agreement also with the results of complementary measurements of specimens that had been oxidized first in  $^{18}\text{O}$  and later in  $^{16}\text{O}$  (not shown).

It has been pointed out previously that lattice diffusion is unlikely and that short-circuit diffusion (of O and/or Al) is the primary transport mechanism in alumina scales.<sup>5</sup> Therefore,  $^{18}\text{O}$  observed near the surface of a specimen oxidized first in  $^{16}\text{O}$  and later in  $^{18}\text{O}$ , indicates outward scale growth. It is due to Al (short-circuit) diffusion up to the oxide/gas interface.  $^{18}\text{O}$  near the oxide/alloy interface indicates oxygen (short-circuit) diffusion down to the alloy/oxide interface. Since the spectra shown in Fig. 3 show an edge at 3.4 MeV and thus indicate outward growth, it can be concluded

that Al is a mobile species in the scale during oxidation. Note that previously reported “marker” experiments using noble-metal markers, positioned on the surface prior to oxidation, incorrectly suggest an inward growth mechanism for alumina scales.<sup>5,10</sup>

The spectra also show that some  $^{18}\text{O}$  has penetrated into the already existing  $\text{Al}_2^{16}\text{O}_3$  scale, thus providing evidence for the mobility of oxygen in the scale during oxidation as well. There are, however, significant differences between the actual  $^{18}\text{O}$  distribution in the scales on the different alloys. Comparison of the profiles of the pure NiAl and 0.07% Y-doped NiAl reveals that in the case of the Y-doped alloy, less  $^{18}\text{O}$  penetrated into the previously formed  $\text{Al}_2^{16}\text{O}_3$  scale during the second oxidation treatment. The rare-earth additions promoted the outward growth. However, both scales

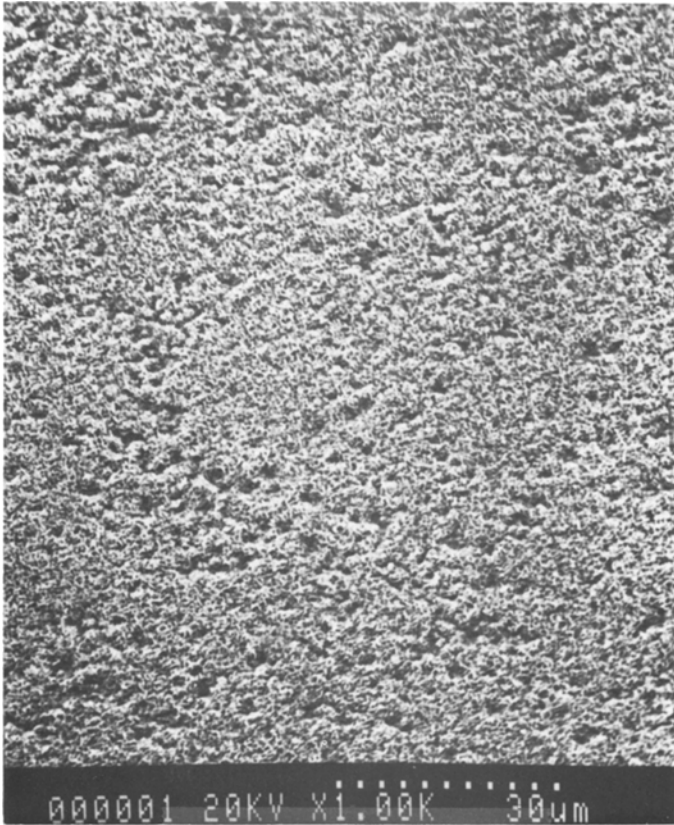


**Fig. 4.** SEM micrograph of NiAl (pure) oxidized for 7 hr at 1270 K (oxide surface).

have about the same thickness, and the scale morphology does not differ significantly either. A micrograph of a scale on the Y-free alloy is shown in Fig. 4.

The  $^{18}\text{O}$  distribution in the scale on the 0.5% Y-doped NiAl shows two  $^{18}\text{O}$  rich regions, one near the scale/gas interface and one near the alloy/scale interface. Although the  $^{18}\text{O}$  distribution in the scale on this 0.5% Y-doped alloy differs from those found on the NiAl and NiAl0.07% Y, the scale thickness and its morphology are about the same again.

SIMS depth-profile measurements were performed on the scales. Figure 5 shows the SIMS depth profile of the oxygen distribution in the alumina scale on NiAl0.5% Y. The same specimen was used for the  $^{18}\text{O}(p, \alpha)^{15}\text{N}$  analysis. The plotted  $^{18}\text{O}$  distribution is the measured  $^{18}\text{O}$  concentration multiplied by two, the plotted  $^{16}\text{O}$  concentration represents the measured value minus the measured  $^{18}\text{O}$  concentration, thus correcting for the use of a 50%  $^{18}\text{O}$  oxygen gas mixture. The agreement between the  $^{18}\text{O}$  distribution in the scale measured this way and the proton-activation depth profile shown in Fig. 3a is excellent. (The depth scale shown in Fig. 5 was deduced from the proton-activation results.)

SIMS imaging was applied to study the lateral distribution of the  $^{18}\text{O}$  in the scale. The  $^{18}\text{O}$  distribution was monitored while eroding the scale down to the alloy/scale interface. Within the lateral resolution of the system in this set-up (1–2  $\mu\text{m}$ ), the distribution of  $^{18}\text{O}$  appeared to be uniform over the scale.

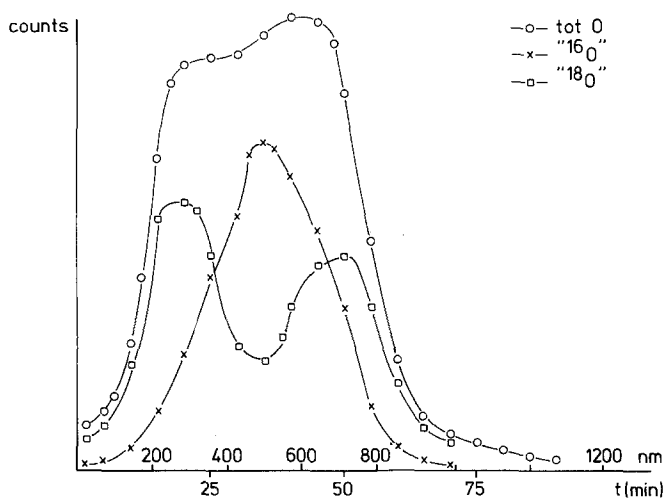


Fig. 5. SIMS profile (prim. beam  $\text{Cs}^+$ , pos. ions detected) of NiAl0.5% Y, oxidized for 1.5 hr in  $^{16}\text{O}$  later for 5.5 hr in  $^{18}\text{O}$  at 1270 K.



Glancing angle X-ray diffraction data show that all investigated scales are mixtures of various transition type alumina phases ( $\theta$ ,  $\delta$ ). But also  $\alpha$  alumina is present in a small amount (weak lines). The scales on the 0.5 and 1.0% Y-doped NiAl also contain some  $Y_2O_3$ .

## DISCUSSION AND CONCLUSIONS

In this study the major contribution of Al transport through the alumina scale during high-temperature oxidation has been demonstrated clearly again. On all the alloys investigated, at least a large part of the scale growth takes place near the gas/oxide interface. This indicates the contribution of Al to the mass transport through the scale. The results of the investigations also clearly show that Y additions influence the mechanism of alumina scale formation of NiAl. Scales on pure NiAl, O, and Al diffusion contribute to the mass transport. On the 0.07% Y-doped alloy an almost pure outward scale growth mechanism was observed. Scale formation on the 0.5% Y-doped alloy occurs near both interfaces. This means that Al diffuses up to the gas/oxide interface and O, simultaneously, diffuses down to the oxide/alloy interface in these scales. If Y-rich segregates are present in the alloy, they are responsible for some internal oxidation. Summarizing we can conclude that small quantities of Y dissolved in the alloy seem to retard the oxygen diffusion and increase the aluminum diffusion through the scale. Higher concentrations of Y result in a higher contribution of oxygen diffusion to the material transport through the oxide. From the literature it follows that the variation of the amount of Y added to an alloy is reflected in different effects on the oxidation mechanism. Most researchers report decreased oxidation rates due to Y additions.<sup>1,13</sup> The effect on the overall oxidation rate is rather small in all cases. We did not study the scale growth kinetics in detail, but our data confirm that Y addition has no dramatic effect on the rate of scale growth.

Because of the fact that Al and O diffusion in the scale are of the same order of magnitude, a change in the mobility of one of them will not have a dramatic effect on the overall rate of scale growth. However, not only the relative contribution of Al and O diffusion should be considered here, but also the diffusion paths and the actual reaction between Al and O is of interest. It cannot be deduced from the data presented above whether Al and O move along the same short-circuit diffusion paths. Some researchers have discussed the diffusion path of Al and O in the scale. Golightly, Stott, and Wood<sup>2</sup> observed ridges on the ( $\alpha$ ) alumina grains at the scale/alloy interface and therefore concluded that oxygen diffused along the grain boundaries and aluminum along short-circuit paths within the grains. In their opinion it is very unlikely that Al and O pass each other while moving

along the same diffusion path. However microscopic observations by Hindam and Smetzer<sup>11</sup> show oxide ridges in the scale extending inward and outward. They suggest that at least part of the Al diffused along grain boundaries. Smialek<sup>3</sup> calls attention to the possibility of grain boundaries as short-circuit diffusion paths in the oxide for aluminum as well. From the observation of whisker growth at the outer surface on transient alumina scales on FeCr alloy (oxidized in air at 1270 K) Moseley *et al.*<sup>12</sup> suggested that a high defect density in the transition alumina allows good cation mobility. It must be stressed here that in the studies cited above a variety of alloys was studied, all at different temperatures, and comparison of the results therefore is rather difficult.

From the results presented in the present paper it is obvious that the alloy (and hence the oxide) composition has a large influence on the oxidation mechanism. Especially in the scales on the 0.5% Y-doped alloy, but to some extent also on the Y-free alloy, we observed scale formation at both interfaces. If part of the Al transport indeed is along grain boundaries, just as the oxygen transport, Al and O must have passed each other. A small addition of Y to the alloy prevents oxygen penetration into the scale. Various TEM and X-ray diffraction investigations<sup>4,12,14</sup> of alumina scales showed the presence of fine Y garnet particles. The presence of such fine Y garnet particles might promote the reaction between Al and O, thus preventing them from passing each other. Since the resulting oxidation mechanism is predominantly outward growth on alloys with a small Y addition, this also suggests that Al moves slightly faster along the grain boundaries than O.

In scales on Y-rich alloys, TEM results have shown an increased number of microvoids.<sup>15</sup> Such microvoids may have provided easy diffusion paths for oxygen only and thus have increased the amount of penetrated oxygen for the 0.5% Y alloy. Because a large part of the scale formation is at the alloy/scale interface on this 0.5% Y alloy, there is relatively little Al transport through the scale. Therefore void formation at the interface, induced by Al-vacancy condensation, will be reduced. Besides, irregularities at the interface will readily be repaired because the interface is renewed continuously. An improved scale adherence could well be the result. Unfortunately there is no direct evidence to verify these mechanisms.

### ACKNOWLEDGMENTS

The SIMS work of Dr. H. E. Bishop, the X-ray diffraction measurements of Dr. B. A. Bellamy, and the helpful assistance of Mr. F. v. Vliet on the 3MV generator are gratefully acknowledged. One of us (EY) would like to express his gratitude for the hospitality of the Surface Analysis Section of

the AERE in Harwell, Didcot, U.K. and the Physics Department of the University of Utrecht, the Netherlands.

### REFERENCES

1. D. P. Whittle and J. Stringer, *Phil. Trans. R. Soc. Lond.* **A295**, 309 (1980).
2. F. A. Golightly, F. H. Stott, and G. C. Wood, *J. Electrochem. Soc.* **126**(6), 1035 (1979).
3. J. L. Smialek, *J. Electrochem. Soc.* **126**(12), 2275 (1979).
4. T. A. Ramanarayanan, M. Raghavan, and R. Petovic-Luton, *J. Electrochem. Soc.* **131**(4), 923 (1984).
5. E. W. A. Young and J. W. H. de Wit, *Solid State Ionics* **16**, 39 (1985).
6. R. Robin, A. R. Cooper, and A. M. Heuer, *J. Appl. Phys.* **44**(8), 3770 (1973).
7. K. P. R. Reddy, J. L. Smialek, and A. R. Cooper, *Oxid. Met.* **17**(5/6), 429 (1982).
8. E. W. A. Young and J. H. W. de Wit, *Proceedings of the 9th International Congress on Metal Corrosion* (Toronto, 1984), Vol. 4, pp. 50.
9. B. A. Bellamy, UKAEA Rep. AERE-R10687 (Atomic Energy Research Establishment, Harwell, Oxfordshire, 1982).
10. E. W. A. Young, H. E. Bishop, and J. H. W. de Wit, *Surf. Int. Anal.* to be published.
11. H. M. Hindam and W. W. Smeltzer, *J. Electrochem. Soc.* **127**(7), 1630 (1980).
12. P. T. Moseley, K. R. Hyde, B. A. Bellamy, and G. Tappin, *Corr. Sci.* **24**(6), 547 (1984).
13. D. Delaunay, A. M. Huntz, and P. Lacombe, *Corr. Sci.* **24**(1), 13 (1984).
14. J. L. Smialek, *Proc. 42 Ann. Meeting EMSA* G. W. Bailey, ed. (San Francisco, 1984), pp. 594.
15. J. L. Smialek, *J. Electrochem. Soc.* **126**, 2275 (1979).